FUEL PIN PRELIMINARY DESIGN

Nuclear Engineering – Politecnico di Milano

Simone Pagliuca, Tommaso Pirola, Lisa Raffuzzi, Riccardo Ronchi, Darien Shabi

simone1.pagliuca@mail.polimi.it

Course: Nuclear Design and Technologies
Academic year: 2024/2025

ABSTRACT: lorem ipsum dolor sit amet, consectetur adipiscing elit. Donec auctor, nunc nec ultricies ultricies, nunc nunc.

Key-words: Key, Words, Here

CONTENTS

1 INTRODUCTION

This report presents the preliminary design and verification of a fuel pin for a sodium-cooled fast reactor, as specified in the assignment.
The analysis involves calculations for material properties, thermal-hydraulic conditions, and mechanical stress limits.
We verify the robustness of our models and justify the assumptions made throughout the process.

1.1 Problem Description

The fuel pin design problem requires:

- Determining the cladding thickness, fuel-cladding gap size, and plenum height.
- Verifying the design against limits for fuel melting, cladding temperature, yielding, and rupture time.
- Identifying critical aspects if irradiation time is doubled.

The project specifications and material properties are mostly given, whenever we had missing information we either used data from previous the handouts which were provided and regarder a similar reactor, or we found the data from the literature.

1.2 Assumptions

To address the given problem, the following assumptions were made:

Steady State Solution for Gas in Grains:

↪ The rate equation for the gas remaining in the grains (PDE) was solved in steady state conditions, given that we just want to size the plenum for 1-year operation and are not interested in the specific behavior in time of the function.

Fission Rate Calculation:

↪ The fission rate was calculated by using the formula (macroscopic cross section * average flux).

↪ The macroscopic cross section of fission was computed from data taken from the JANIS database.

↪ The average flux was evaluated considering power and flux profile to be equal.

Material Properties and Geometry:

↪ Material properties are temperature-dependent and were modeled using provided empirical correlations.

↪ Axial power and neutron flux profiles remain constant over time.

↪ Initial helium pressure and temperature in the fuel-cladding gap were assumed as specified.

↪ Simplifications in geometry, such as neglecting axial deformation, were made to ease computation.

2 VERIFICATION OF MODELS

Each part of the analysis code has been checked to confirm it behaves as expected under the defined conditions.

2.1 Thermal-Hydraulics Analysis

Preliminary checks were conducted on coolant properties.

Density, viscosity, and thermal conductivity were validated at the coolant inlet temperature.

The heat transfer coefficient between the coolant and cladding was computed using Nusselt number correlations.

Figure 1 shows the axial power profile. the computed heat transfer coefficient in cold geometry was $\alpha_{coolant} = 139.98 \frac{kW}{m^2 K}$.

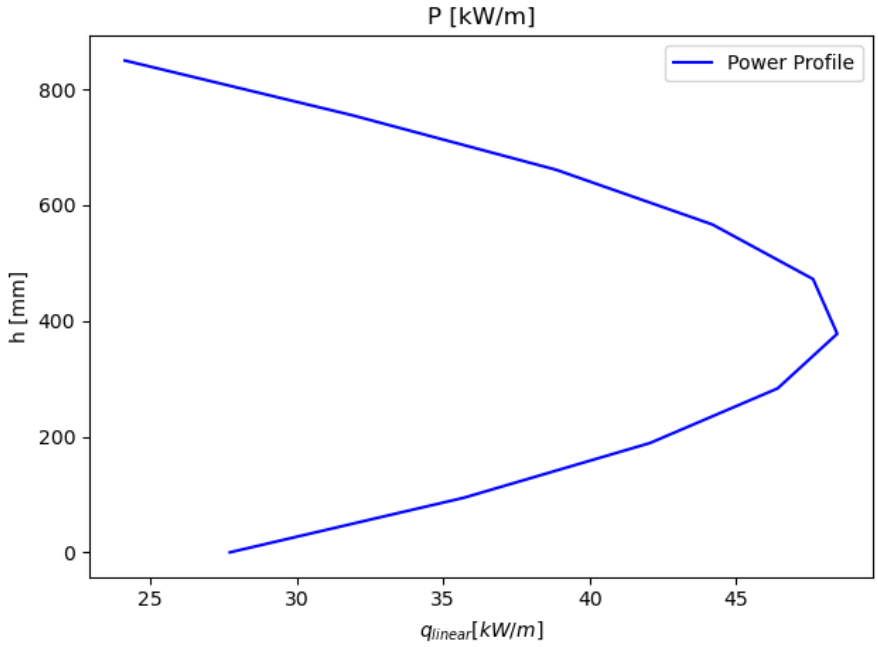

Figure 1: Thermal-hydraulics analysis results.

2.2 Temperature Profiles

Radial and axial temperature profiles were computed for the cold geometry to check if the shape of the profile made sense and if the values were reasonable.

We create a temperature map of the fuel rod. For every node along the axial direction, we first compute the temperature increase in the coolant due to the heat generated in the fuel. From this we compute the temperature at the coolant cladding interface using the heat transfer coefficient (computed by given correlations). For the cladding again we approximate to a linear temperature profile and compute the temperature at the cladding gas interface. Then for the gap and the fuel we compute several temperature points along the radius, at every step the properties are updated to the temperature of the previous step. The inner void is at the same temperature as the inner surface of the fuel.

The results provided an initial validation of the temperature distribution behavior before further analysis.

Figure 2 illustrates the temperature along the axis, at the interfaces, while Figure 3 shows the radial temperature profiles at the bottom, middle and top of the fuel rod.

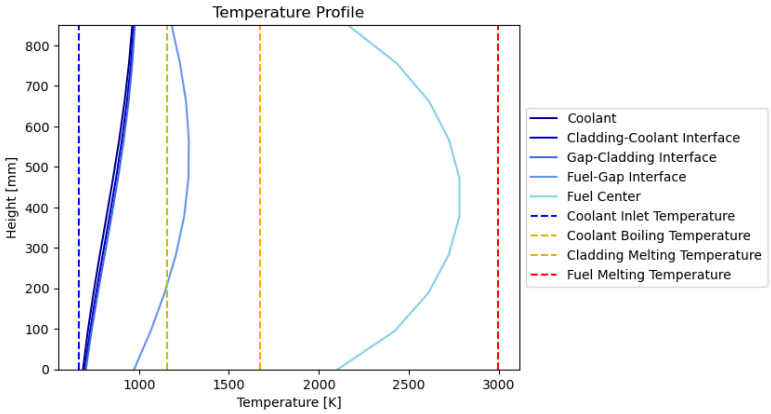

Figure 2: Axial temperature profile for cold geometry.

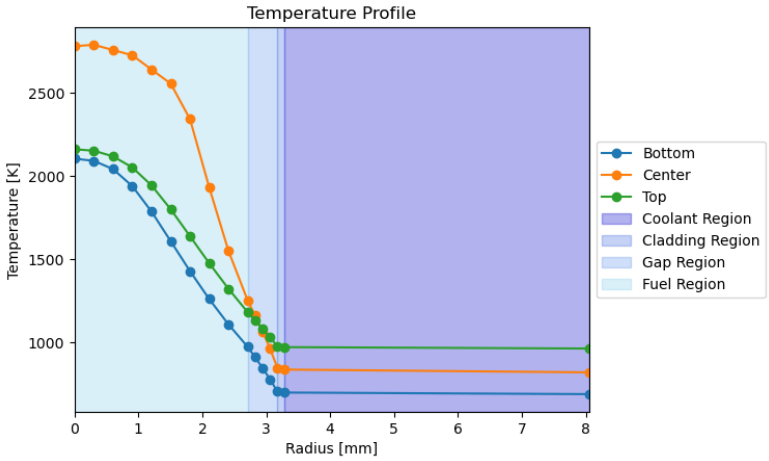

Figure 3: Radial temperature profile for cold geometry.

2.3 Thermal Expansion Analysis

The fuel and cladding form a coupled system, with the gap between them playing a crucial role in heat transfer, mechanical interactions, and safety. Accurate evaluation of thermal expansion is essential to ensure efficient operation and structural integrity of the reactor core. The calculations consider material-specific thermal expansion coefficients and the temperature distributions derived from reactor operational data.

2.3.1 Axial Temperature Profile of the Fuel and Axial Profile of Fuel Radius (Cold vs. Hot Geometry)

The fuel's axial temperature profile under hot operational conditions is shown in Figure 4. It illustrates the temperature distribution along the fuel height, which is essential for understanding thermal stresses and expansion. We can see that the material's expansion follows perfectly the fuel temperature profile (Figure 5).

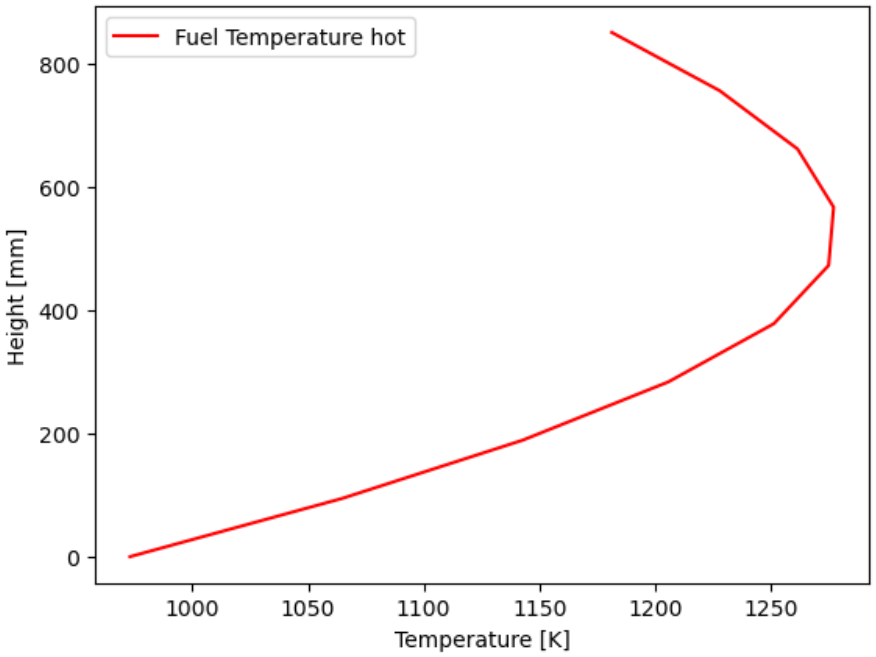

Figure 4: Axial temperature profile of the fuel under hot conditions.

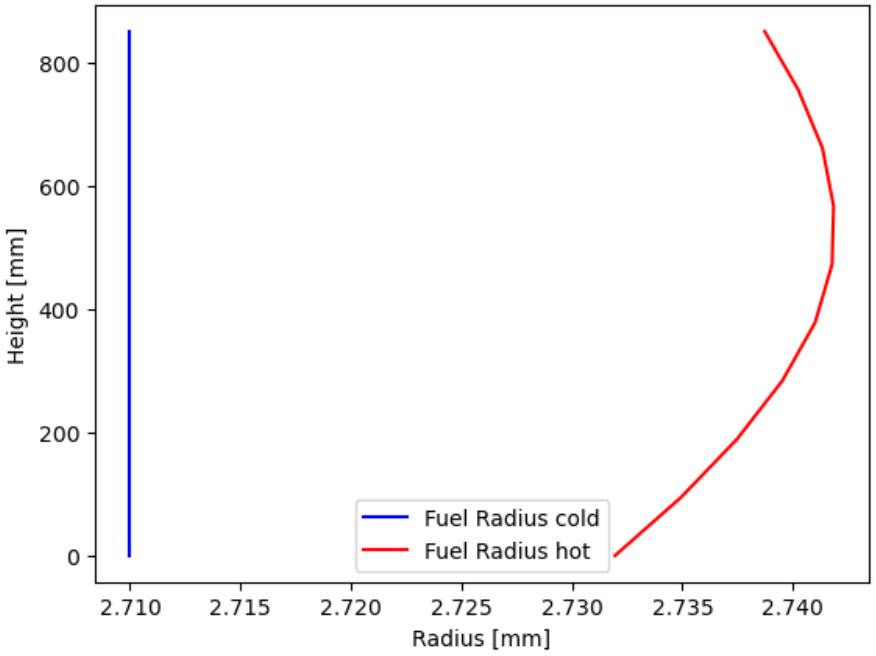

Figure 5: Axial profile of fuel radius (cold vs. hot geometry).

2.3.2 Axial Temperature Profile of the Inner and Outer Cladding (Cold vs. Hot Geometry)

The inner and outer temperature profiles of the cladding show the thermal distribution along its axial height. These graphs highlight the uniform expansion of the cladding along its height (Figure 6). The temperature difference between the inner and outer part is uniform, as shown in Figure 7.

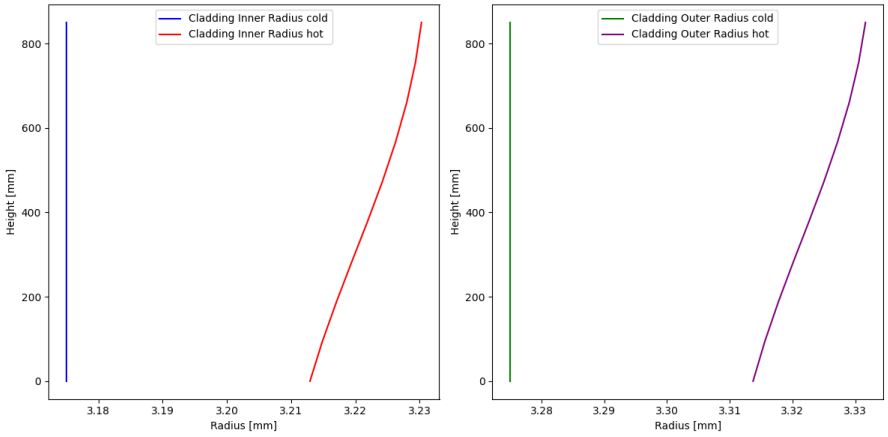

Figure 6: Axial temperature profile of the cladding (cold vs. hot geometry).

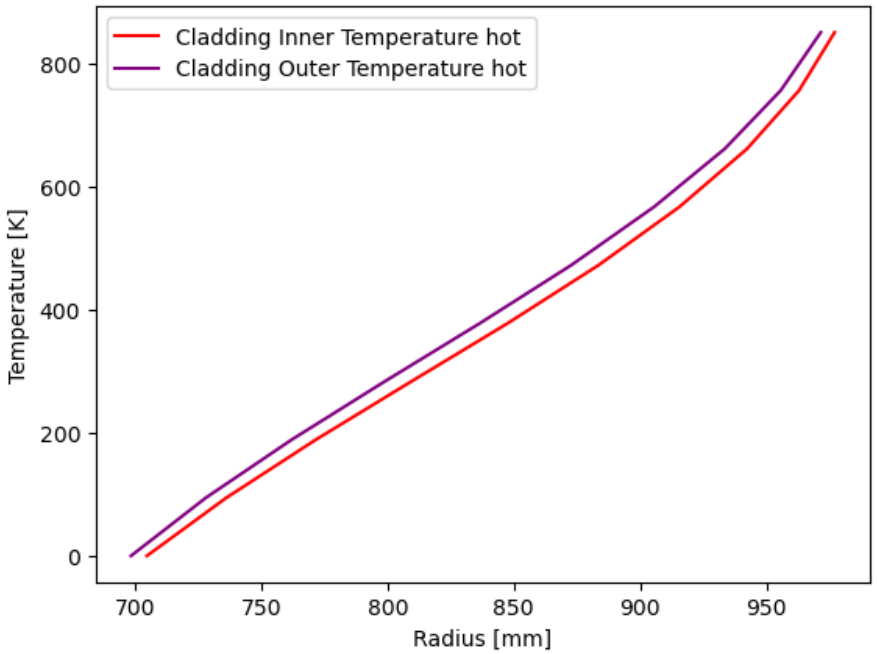

Figure 7: Axial profile of cladding radius (cold vs. hot geometry).

2.3.3 Gap and Cladding Thickness Along Axial Height

The evolution of the fuel-cladding gap due to differential expansion is shown in Figure 8. This parameter directly impacts heat transfer efficiency and mechanical interactions in the reactor core. The change in cladding thickness with temperature is minimal compared to the change in radius. However, it is still a key parameter for evaluating structural integrity.

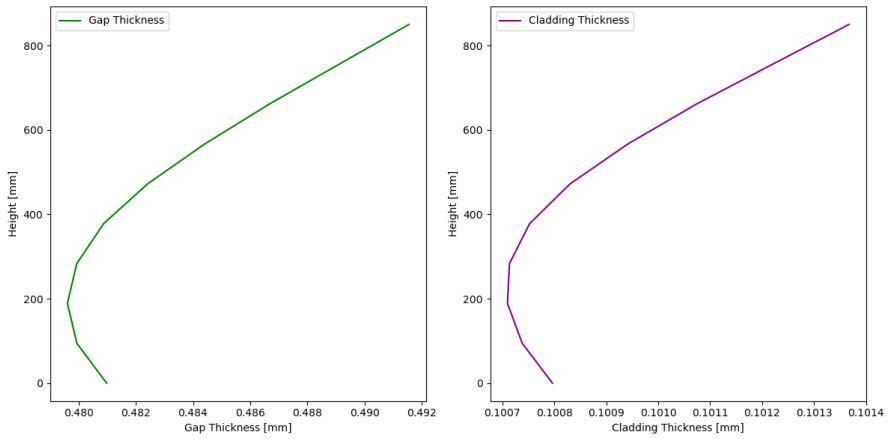

Figure 8: Gap and cladding thickness along the axial height.

2.3.4 Discussion

As expected, the fuel's thermal expansion is more pronounced due to its higher temperature gradient compared to the cladding. The gap between the fuel and cladding decreases, which improves thermal coupling but must be managed carefully to avoid mechanical interactions that could compromise the system's integrity.

2.4 Void Swelling

A correlation for the volumetric void swelling of the cladding was given. We assumed the swelling to be isotropic and therfore the radial expansion is $\frac{1}{3}$ of the volumetric expansion. Figure 9 shows the swelling of the cladding along the axial direction. We can see that, as expected, the swelling is only contained within a range of temperature: too low and no swelling, too high and the mobility is high enough that recombination prevails.

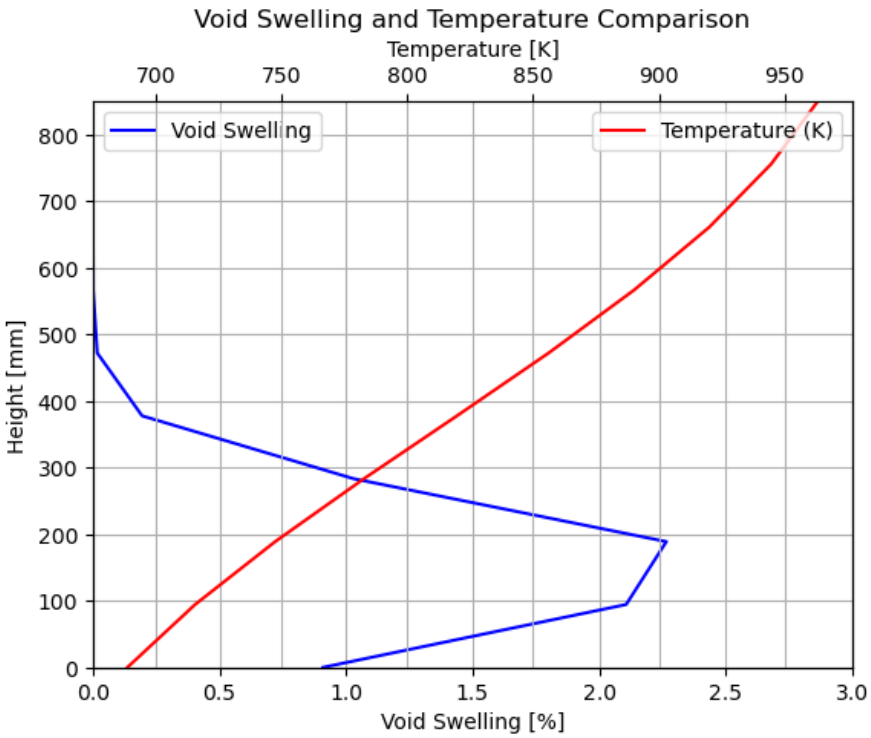

Figure 9: Cladding swelling due to void formation.

2.5 Fission Gas Behavior

Rate theory equations were solved to estimate fission gas production and release over the fuel cycle.

The rate equation for the gas remaining in the grains was solved under steady state conditions, given that we are only interested in sizing the plenum for 1-year operation.

The fission rate was calculated as the product of the macroscopic cross section and the average flux.

The macroscopic cross section was obtained from data in the JANIS database, and the average flux was estimated by assuming the power and flux profiles were equivalent.

The concentration profiles are shown in Figure 10.

Figure 10: Fission gas concentration profiles.

2.6 Restructuring

After transitioning from cold geometry to hot geometry and evaluating the thermal expansion we have to take in account the fuel restructuring process. We make some assumption about columnar and equiaxed region-radii, as well as on densities in different regions. We set the temperature boundaries for columnar ragion at 1800°C and at 1600°C for equiaxed region, according to Holander's book. Regarding the densities, we consider that in the As-fabricated region the density remains the same, while in the equiaxed a percentage of TD of 95First of all, we evaluate columnar and equiaxed radii respectively at 1800°C and 1600°C as we said, based on a temperature map. This map provides the temperature at different heights along the fuel pin, using a precise function that allows us to determine the temperature at any position in the 3D model previously developed Once columnar and equiaxed radii are determined, we have to evaluate the void radius. The As-fabricated region is only the remaining potion of the fuel outer radius after subtracting the equiaxed region. Using this simple correlation to make a possible solution of void formation:

$$R_{void} = \sqrt{R_{\text{col}}^2 - R_{\text{eq}}^2 \cdot \left(\frac{\text{Density}_{\text{AS}}}{\text{Density}_{\text{col}}}\right) + (R_{\text{eq}}^2 - R_{\text{col}}^2) \cdot \left(\frac{\text{Density}_{\text{eq}}}{\text{Density}_{\text{AS}}}\right)} \tag{1}$$

At end, there is the plot of the fuel element: height vs Radius. We want to show the restructuring phenomenon and highlight the contributions' dependence on the axial position-z of the fuel pin Figure 11 shows

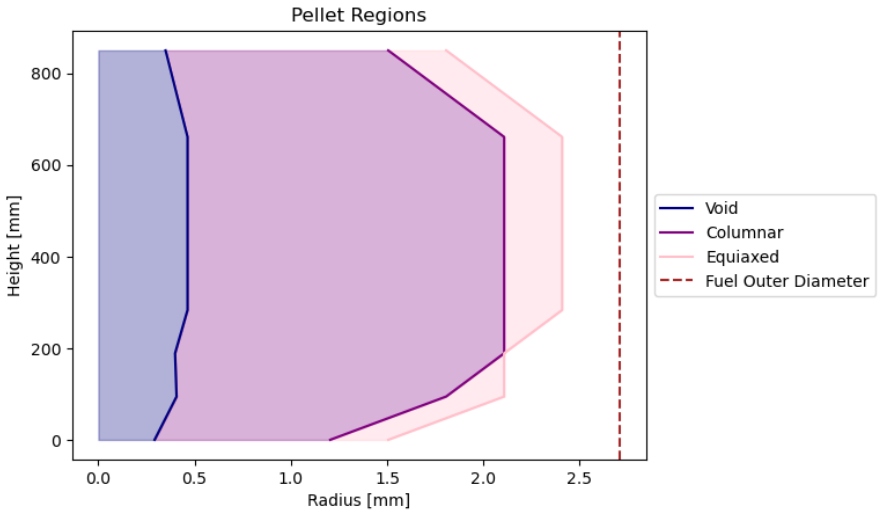

Figure 11: Cladding swelling due to void formation.

2.7 Stress Analysis

Figure 12 shows

Figure 12: Cladding swelling due to void formation.

3 OTHER EFFECTS

Additional phenomena, such as plutonium redistribution and helium embrittlement, are considered to provide a broader understanding of the fuel pin's behavior.

3.1 Plutonium Redistribution

As a consequence of restructuring, it became necessary to investigate the phenomenon of Plutonium redistribution. During restructuring, as observed, the formation of distinct zones occurs within the fuel element:

- Central void
- Columnar grains (pores migrate, and mass is displaced outward)
- Equiaxed grains (caused by grain growth at high temperatures)
- As-fabricated (temperature is too low to cause changes)

These different zones are characterized by differences in density and, consequently, porosity. This is due to the densification of the fuel, reaching up to 98-99% of TD.

Due to this phenomenon, the density variation results in a change in Plutonium concentration across the different zones of the fuel, which initially had a uniform concentration of 29%. There is an enrichment of Plutonium in the central (columnar) zone, followed by an initial decrease reaching a minimum value, which corresponds to a depletion in the equiaxed zone. In the as-fabricated zone, the concentration stabilizes back to the initial value. The redistribution of Plutonium thus affects part of the fuel element and is a consequence of the high activation energy of Plutonium.

To evaluate how Plutonium redistribution varies following the phenomena of thermal expansion and fuel restructuring, we used the following formula, as provided in the handouts (Hot Effects Analysis, V):

$$\frac{q'''(r)}{q_0} = \frac{c(r)}{c_0} = 1 + D\left\{\exp\left[-2\alpha\left(\frac{r-r^*}{R_{\text{fo}}}\right)\right] - 2\cdot\exp\left[-\alpha\left(\frac{r-r^*}{R_{\text{fo}}}\right)\right]\right\} \tag{2}$$

where:

- $D = 0.01$ (from handouts),
- α is equal to 10 (from handouts),
- r^* is an empirical constant set to $0.207 \cdot R_{\text{fo}}$, a value that ensures the conservation of Plutonium during redistribution,
- $C(r)$ is the radial Plutonium concentration [g/cm^3],
- c_0 is the initial Plutonium concentration.

Graphically, this result clearly illustrates all the phenomena associated with Plutonium redistribution.

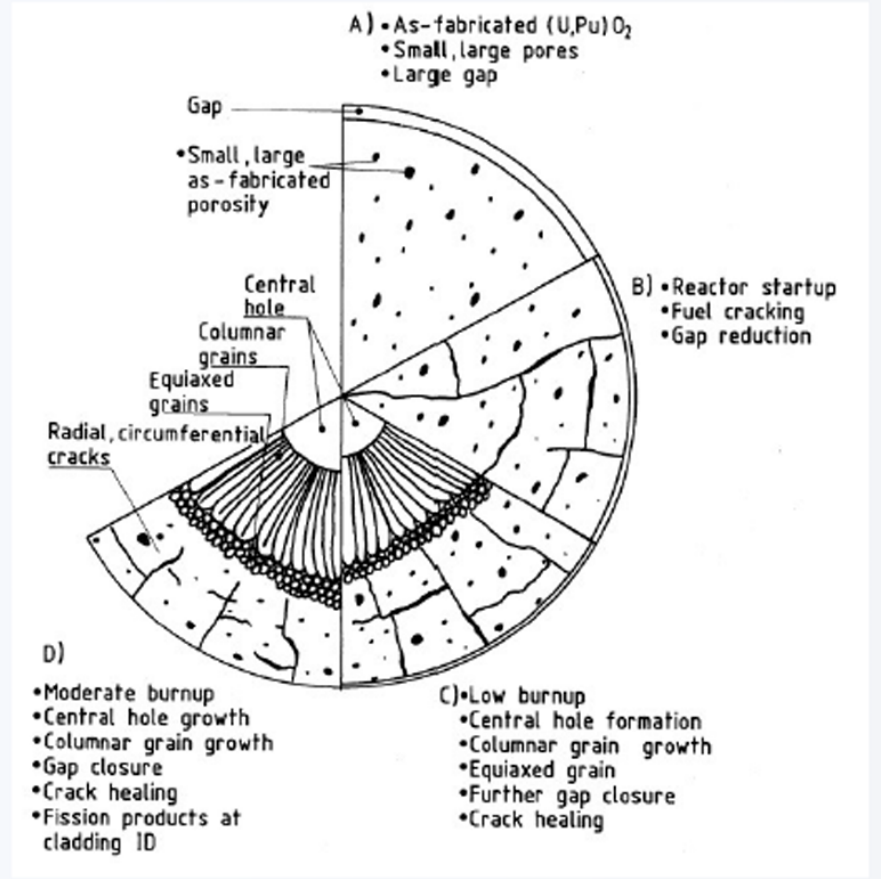

Figure 13: Restructuring of fuel elements and formation of zones during irradiation.

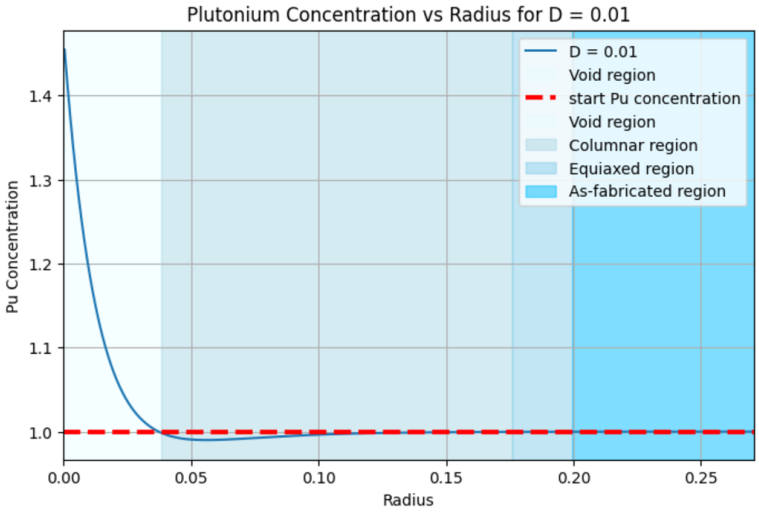

Figure 14: Radial distribution of Plutonium concentration (relative to starting concentration) within the fuel structure.

3.2 Helium Embrittlement

Figure 15 shows the swelling of the cladding along the axial direction.

Figure 15: Cladding swelling due to void formation.

4 DESIGN RESULTS AND CONCLUSION

The study presents the design outcomes, their implications, and the conclusions drawn on the feasibility and safety of the proposed design.

4.1 code

After this the different pieces of code had to be adapted to properly work toghether, the result of this was compared to the previous work to ensure that nothing was ”corrupted” during the process.
We have then created a code that takes as input a value of cladding thickness and plenum height and will iterativly undergo the computation until the temperature map converges to a stable solution.
To dimensition these two quantities a previously implemented genetic algorithm was used.

4.2 Results

All of the code can be found in the following Github repository: